

Numerical Computing of Collection Efficiency for Wire-Duct ESP in Babylon Cement Plant

FADHIL K. FULIFUL, ANAAM A.HAMOOD

Department of Physics, College of Science, University of Karbala, Karbala, Iraq

E-mail: Fadhil.Khaddam@yahoo.com

Abstract

This paper presents the evaluation of performance of wire-duct electrostatic precipitators (WDESP) in Babylon cement plant. Finite Difference Method (FDM) and FORTRAN programs version 95 are used to compute the potential contours and electric field along the distance between the discharge electrode and collecting plates for different values of wire radius, charge density and current density also calculated. The voltage-current (V-I) characteristics are evaluated by solving Poisson and current continuity equations simultaneously using iteration method. A good agreement is obtained between the present model predictions and the experimental particle collection efficiencies obtained from the literature. It is expected that the present model can be used for diagnostic the problems which can be happen in ESP of Babylon cement plant.

Introduction

Air pollution can affected our health in many ways, also damages our environment, can also impact the Earth's climate, and consists of gas and particle contaminants that are present in the atmosphere. Generally, emissions come from the fuel combustion (such as power plant, petroleum refineries, and cement plants).

Electrostatic precipitator (ESP) is one of the most common control device used to control fly ash emissions from the industrial plants such as purifying the flue gases from coal burning or cement production plants. Research programs of the Environment Protection Agency (EPA) are providing data and technical support for solving environmental problems today and building a science knowledge base necessary to manage our ecological resources wisely, understand how pollutants affect our health, and prevent or reduce environmental risks in the future [1-2]. The most common type for an electrostatic precipitator is the wire-duct or wire plate. The performance of (ESP) can be determined by means of voltage-current V-I characteristics which help in predicting the electrical problems that occur under clean air conditions in precipitator. Also, they play an important role in predicting the performance of the (ESP) in the design stage for different mechanical input data such as wire radius, wire-to-wire spacing and wire-to-plate spacing, etc. [3-6]. The basic

principles governing the operation of electrostatic precipitators as follows: when a large voltage is applied between the electrodes; gas particles are passed through an electric field where they are initially charged by means of a corona discharge [7-10] therefore electrons are emitted from discharge electrodes and collide with airborne particles then ionize them during migrating toward collecting plate to form a continuous layer that can be effectively removed by mechanical rapping or vibrating of the plate.

In addition, there are many investigations about the electrical problem in ESP. Estimation the V-I characteristics of a wire-plate high-voltage configuration system, prediction of spark-over voltage and ion charge density at corona edge are calculated, using a new equation, which was developed by dimensional analysis to compute the number of grid points [11]. Adopted a finite element method (FEM) to calculate the potential and field distributions along the (WDESP) axis (between the central wire and collecting plate) and mid-way between wires and collecting plate agreed well with those published before, also the V-I characteristics and the current density distributions along the collecting plate for both single- and three-wire precipitators have been calculated [12]. The collection efficiency of a (WDESP) under dust loading conditions have been estimated, the finite element method (FEM) and a modified method of characteristics are used to solve Poisson's equation and to satisfy the current continuity condition, respectively depending on iterative method and the effect of varying the dust particle concentration on the computed efficiency is demonstrated [13]. A developed algorithm for combined finite element based method (FEM) and a modified method of characteristics (MMC) is employed [14] for the analysis and computation of the current density profiles, corona current and hence corona power loss associated with (WDESP) under particle loading conditions, a proto-type design that represents a WDESP, which has been fabricated at the research institute of KFUPM (RI-KFUPM), is used to test the developed algorithm by varying different geometrical parameters. At Raichur thermal power station, in India, [15] reported a new approach based on (FDM), for the prediction of electrical conditions and voltage-current characteristics in a dc energized (WDESP) with and without dust loading, this simple method gives sufficiently accurate results with reduced mesh size, the results for simulation were validated with published experimental. [16] Proposed four types of collection plate configurations to study the V-I characteristics of a pin-plate system. The experimental results showed that clean filter media on dust collection plate does not have evident effect on the V-I characteristics of electrostatic region while the dirty filter media reduce current density because of the high resistance in the other hand the thick fly ash, cake layer doesn't have noticeable increase on current density. [17] Investigated the electrostatic characteristics of different filter media types used in the hybrid filtration system. The V-I characteristics of needle-plate system, the collection plate of which is covered by filter media, were measured. Seven types of filter media and collection plate including iron plate, iron grid and activated carbon layer were considered. A numerical model was developed on the ESP's at Karbala cement [18], this model describe the voltage-current characteristics without and with loading dust, in the second case, V-I illustrated effect of back corona with different values of both resistivity and dust layer, another way for detecting back corona between the dust layer and the collecting plate is the value of electric field between them. The effect of back electrostatic-field due to particle buildup on the collection plates of an electrostatic lunar dust collector ELDC was investigated [19] using a discrete element method DEM to track particle trajectories,

and sensitivity analyses were conducted for the concentration of the incoming particles, the model applicable for an ELDC of any size. The obtained results from tracking particle trajectories confirmed the formation of the circulation regions in proximity of the collection plate.

In this paper an iterative procedure is based on (FDM) and FORTRAN programs which are using for solving both Poisson's and current density continuity equations simultaneously in order to investigate potential, electric field, and charge density. V-I characteristics of (WDESP) of Babylon cement plant under clean air condition are also computed. The performance of an (ESP) can be predicted by the V-I characteristics for different input data such as wire radius, the numerical solution can be used as a tool for prediction the electrical problem properly occur in ESP of Babylon cement plant. The mathematical model can be employed for simulation of dust the additional data required are radius, specific gravity and relative permittivity of the dust particle, dust concentration, air viscosity, mean ion free path and back corona.

Mathematical model

There are some assumptions made for the mathematical analysis Dc voltage is applied to the wire, the discharge electrode is a round and smooth wire, there is no dust in the inter-electrode region, the mobility of charge carriers is constant, neglect the ion diffusion, the same diameter for all particles and electric field on the wire is equal to the corona onset gradient given by Peek's formula [21]

$$E_0 = 32.3 * 10^5 \delta + 0.846 * 10^5 \sqrt{\delta/R_0} \quad (1)$$

Where δ is the relative air density and R_0 the radius of the discharge wires. The various boundary conditions for potential u and the problem domain are shown in Fig. (1):

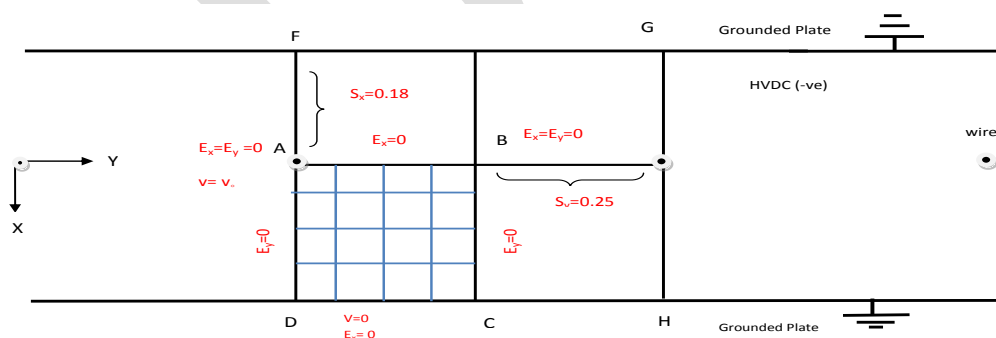


Fig.(1) One quarter section (ABCD) of wire duct ESP for Problem domain in Babylon cement plant

$u|_A = u_0$ on the discharge wire, $u|_{DC} = 0$ at the ground plates,

The electric field at the corona electrode is E_0 .

A first estimate of the voltages (u) at the grid points are obtained using Cooperman's equations [22].

$$u(x, y) = u_0 \frac{\sum_{m=-w}^w \ln \left\{ \frac{\cosh \left[\frac{\pi(y-2ms_y)}{2s_x} \right] - \cos \left(\frac{\pi x}{2s_x} \right)}{\cosh \left[\frac{\pi(y-2ms_y)}{2s_x} \right] + \cos \left(\frac{\pi x}{2s_x} \right)} \right\}}{\sum_{m=-w}^w \ln \left\{ \frac{\cosh \left(\frac{\pi m s_x}{s_x} \right) - \cos \left(\frac{\pi r}{2s_x} \right)}{\cosh \left(\frac{\pi m s_x}{s_x} \right) + \cos \left(\frac{\pi r}{2s_x} \right)} \right\}} \quad (2)$$

where, u_0 is the voltage applied on the wire, x and y are the co-ordinate position in meters measured with the wire as origin, s_x is wire to plate spacing, s_y is half wire to wire spacing, r is the radius of the wire, and w is the number of wires.

Solution to Poisson's equation and current continuity equation's:

Finite different method (FDM) is elected to solve Poisson and current continuity equations simultaneously. Due to the double symmetry in the precipitator geometry shown in Fig.(1), it is sufficient to study the mathematical model for one quarter of the regions between a pair of the wires and the plates bounded by the area (ABCD).

Poisson's equation is given by:

$$\nabla^2 u = -\frac{\rho}{\epsilon_0} \quad (3)$$

Where, ρ is the charge density and ϵ_0 is the permittivity of free space.

The electric field related to the voltage as follow:

$$E = -\nabla u \quad (4)$$

Calculation of space charge density at the wire is essential as it is given as one of the boundary conditions. Approximating the plasma region surrounding the electrical discharge as cylindrical can be evaluated in terms of estimation average current density J_p as [6]

$$\rho(i, j) = \frac{2s_y J_p}{\pi b E_0 r_i} \quad (5)$$

J_p = estimation current density along the plate (A/m^2) input data, b = effective mobility of charge carriers ($m^2/V \cdot s$) and $r_i = (1mm)$ radius of the plasma region round the discharge electrode (m) and approximately equal to the wire radius of discharge electrode, E_0 is calculated from eq.(1)

In two dimensions such as in Fig.(2) equation (3) becomes:

$$\frac{\partial^2 u}{\partial x^2} + \frac{\partial^2 u}{\partial y^2} = -\frac{\rho}{\epsilon} \quad (5)$$

the voltage at any point in a grid shown

In Fig. (2) can be calculated using second

order finite differences

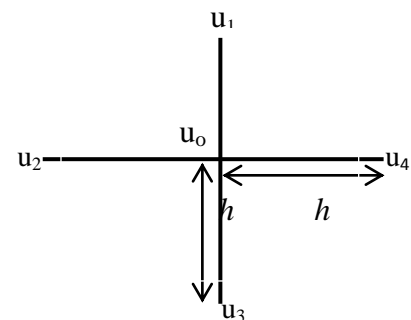


Fig.(2) grid points

bycentral difference method

$$\frac{\Delta^2 u}{\Delta^2 x} = \frac{u_4 + u_2 - 2u_0}{(\Delta x)^2} \text{ and } \frac{\Delta^2 u}{\Delta^2 y} = \frac{u_1 + u_3 - 2u_0}{(\Delta y)^2} \quad (6)$$

Substituting eq. (6) in (5) and letting $(\Delta x = \Delta y = h)$ obtained

$$u_0 = \frac{1}{4} \left[(u_1 + u_2 + u_3 + u_4) + \frac{h^2}{\epsilon_0} \rho \right] \quad (7)$$

In applying the methods of finite differences, the solution of domain into a finite number of meshes as shown in Fig.(3)

With reference to Fig.(2) equation (7) becomes

$$u(i, j) = \frac{1}{4} \left[u_{i,j+1} + u_{i-1,j} + u_{i,j-1} + u_{i+1,j} + \frac{h^2 \rho}{\epsilon_0} \right] \quad (8)$$

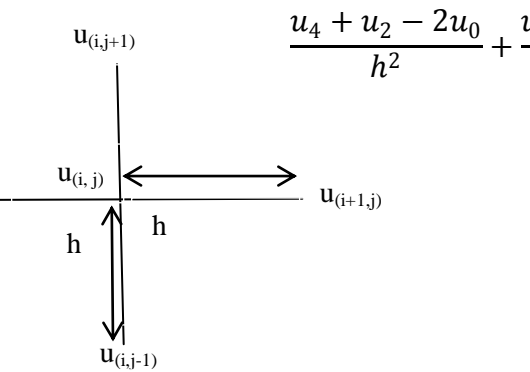


Fig.(3) square meshes

From equation (8) it is clear that voltage at the central node is the mean of the voltages at the other four nodes, the values of potential at all the point in the grid can be calculated by repeating the central node at another point.

The current continuity equation is given by:

$$\nabla \cdot J = 0 \quad (9)$$

The relation between current density and electric field is given by:

$$J = \rho b E \quad (10)$$

From eq. (9) and (10) we can get:

$$\begin{aligned} \nabla \cdot (\rho b E) &= 0 \\ (\rho b) \nabla \cdot E + b(E \cdot \nabla \rho) + \rho(E \cdot \nabla b) &= 0 \end{aligned}$$

The last term will be zero since b is a constant, rewriting the same

$$(\rho b) \nabla \cdot E + b(E \cdot \nabla \rho) = 0 \quad (11)$$

The solution for the current continuity equation is obtained using FDM as

$$\frac{\partial \rho(i,j)}{\partial x} = \frac{\rho(i,j) - \rho(i-1,j)}{\Delta x} \quad \text{and} \quad \frac{\partial \rho(i,j)}{\partial y} = \frac{\rho(i,j) - \rho(i,j-1)}{\Delta y} \quad (12)$$

By substituting equation (12) in equation (10) and let $(\Delta x = \Delta y = h)$ we get

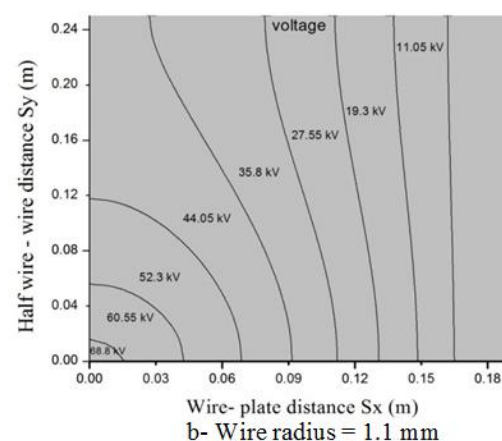
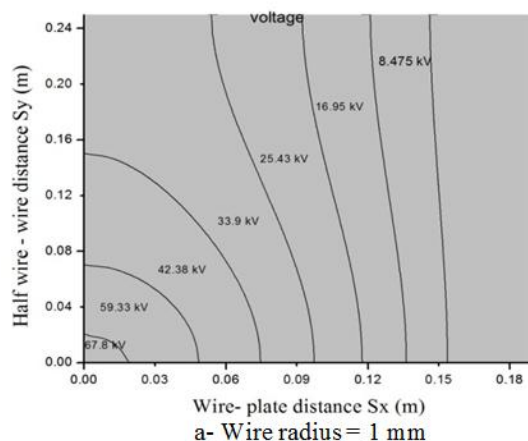
$$\frac{h}{\epsilon_0} \rho_{(i,j)}^2 + (E_x + E_y) \rho_{(i,j)} - (\rho_{(i-1,j)} E_x + \rho_{(i,j-1)} E_y) = 0 \quad (13)$$

Now, current density J at the plate can be calculated by solving eq. (13) after finding the value of charge density [2, 6]:

$$J_{avg} = \frac{1}{n} \sum_{j=1}^n (\rho b) E_x \quad (14)$$

Results and discussions:

The solution of Poisson's and current continuity equations are described simultaneously in the preceding section using a computer program. The distribution of potentials and electric field are estimating. Space charge and current densities at all points of the grid which consists of (22×22) also calculated using FDM with FORTRAN program. The input data required to the program as follow: applied voltage at the wire is 45 kV, wire radius is 1mm, half wire to wire spacing 25 cm, wire to plate spacing is 18 cm, effective mobility of the charge carriers is $2 \times 10^{-4} \text{ m}^2/\text{v.s}$, air density factor at NTP; $\delta = 1.0$ and roughness factor of the wire $f = 1.0$. The first step of the program after input data is the computation of potential distribution according to the Cooperman's equation (1). When the electric potential can be estimation, the electric field at all point in the grid also known by the famous relation (equation 4) and the boundary condition which is depended in this paper. The space charge density at discharge wire computed due to equation (5) and using equation (13) to evaluate the space charge density at all point in the grid of domain. The another step is to determine the electric potential distribution at the quarter section of ESP using the equation (8) by dividing the area at four region (see fig.1), first is the line AD, the second is line AB, third is line BC and the fourth is the core of the configuration, the condition for this step is the difference between the value calculated by equation (2) and (8) is less than one volt using iterative procedure. The last step for the program is calculating current density by using equation (13), and compared the prediction value of current density with estimated value as input data and the comparison satisfied the condition "The difference between two values are less than 3%". While the values of potential and current density are computed the V-I characteristics are obtained and the efficiency of ESP can be predicted. The condition of potential difference calculated in equations (2 and 8) has a close agreement at lower applied voltage and larger than one volt at higher voltage.



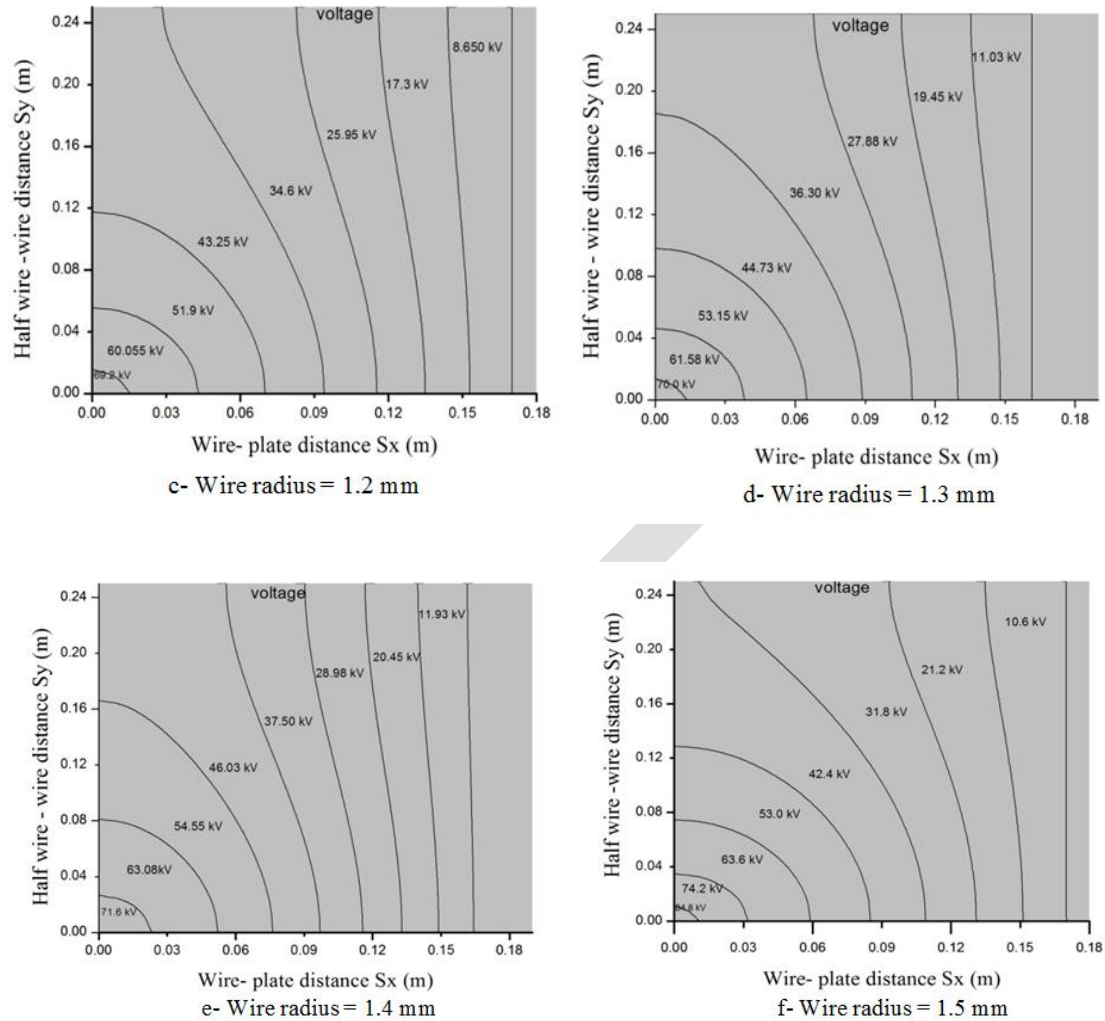


Fig.4 (a, b, c, d, e, f) Potential contours for a quarter section (Fig.1) for various wire radius.
Input data: $S_x = 18$ cm, $S_y = 25$ cm, $b = 2 \times 10^{-4} \text{ m}^2/\text{v. s}$, $f = 1.0$; $\delta = 1.0$.

Fig. (4) Shows the contour potential distribution for a quarter sections of the ESP of Babylon cement plant, the boundary condition for solution Poisson's equation is valid when we see the equipotential surface. It is clear that the voltage at higher value at the wire discharge and began to decrease when we move far away from it that equal zero to collecting plates. The contour potential distribution behavior the same manner at different values of wire radius but the applied voltage on the discharge wire is increased $u=67.8\text{kV}$, $u=68.8\text{kV}$, $u=69.2\text{kV}$, $u=70.0\text{kV}$, $u=71.6\text{kV}$, $u=84.8\text{kV}$ for fig.3 (a, b, c, d, e, f) respectively. The effect of varying the discharging wire radius usually lead to increasing of applied voltage, and continuous increasing in wire radius making spark and erosion destroy the discharge wire therefore the designer must be carefully for choosing the radius of the discharge wire. The tool used to determine the sparking is V-I characteristics.

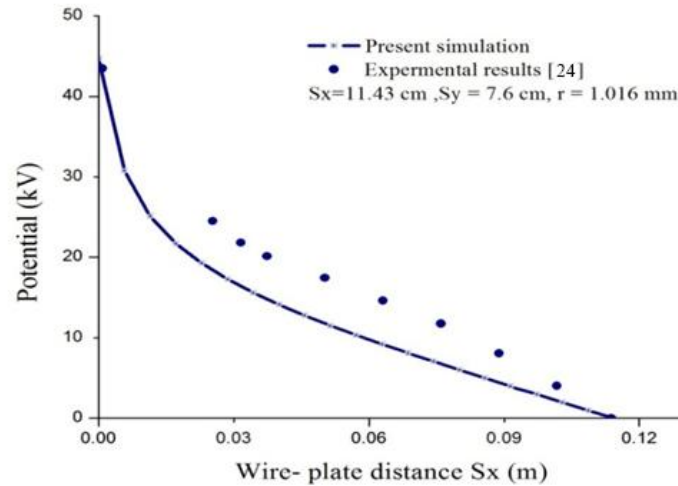


Fig.(5) Experimentally and calculated results of potential distribution along wire – plate.

In fig.(5) It is clear that comparison between computed and experimental of potential distribution along wire – plate show satisfactory agreement and this agreement illustrated the efficiency of the proposed procedure. The applied voltage is (45kV) at discharge wire and zero at the collecting plate which is assurance that corona discharge occurs.

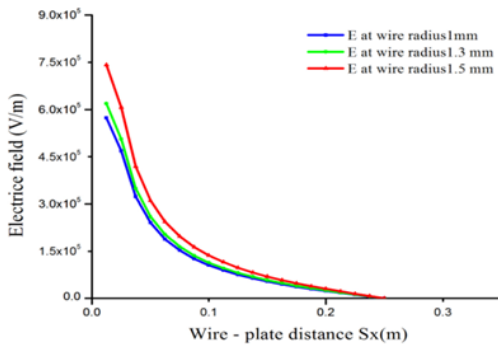


Fig.(6)E- field distribution along S_x (m)

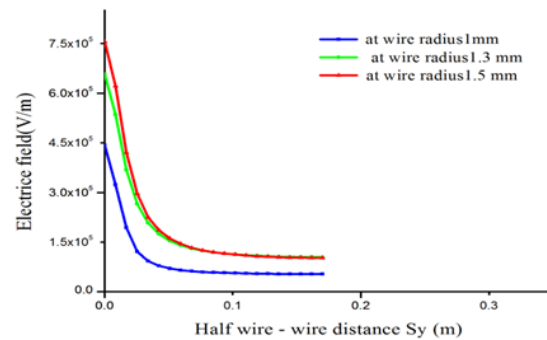


Fig.(7)E- field distribution S_y (m)

Fig's. (6, 7) electric field distribution for various wire radius
input data ($S_x=0.17$ m, $S_y=0.25$ m, $v=45$ kV, $b=2 \times 10^{-4}$ m²/v.s).

The electric field distribution is shown in fig.(6) show that there are strong electric field (5×10^5 V/m) around the region of high voltage electrode(plasma region) and decrease slowly along the x-axis(S_x) until the value is equal zero due to the earth collecting plates. The comparison between three curves illustrated the large radius of discharge electrode give high electric field but another increasing (larger than 1.5 mm) lead to spark. In the same way we can discuss the distribution of electric field along y-axis (S_y)fig.(7) but we see that minimum value (5×10^4 V/m) of electric field does not equal zero because the half distance between the discharge electrodes .

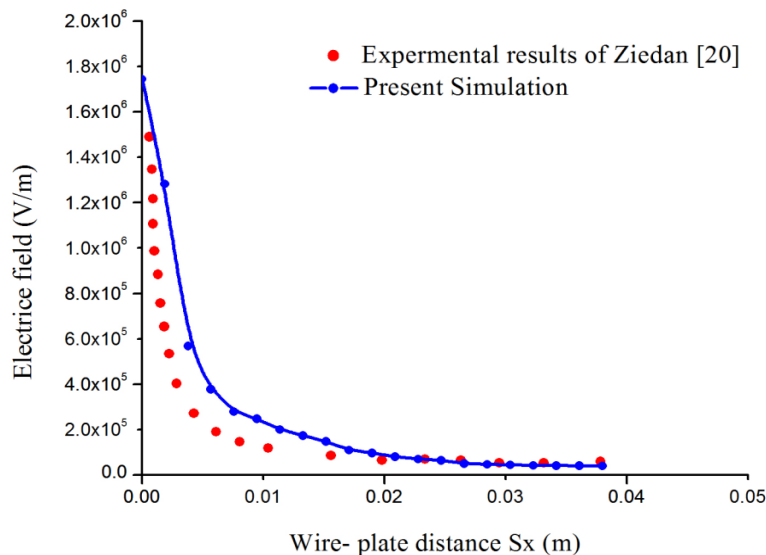


Fig.(8)the comparison between experimental and calculated results of electric field distribution along wire-plate distance, input data: $S_x = 3.8$ cm, $S_y = 7.6$ cm, $r = 0.8$ mm.

Fig.(8) Show the comparison between experimental and calculated results of electric field intensity distribution along the (x-axis) ,it is clear that experimental results reported by Zeidan [20] close to our simulation at the same input data.

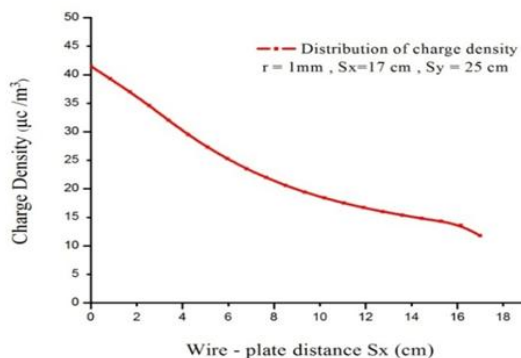


Fig.(9) Charge density distribution along wire-plate distance

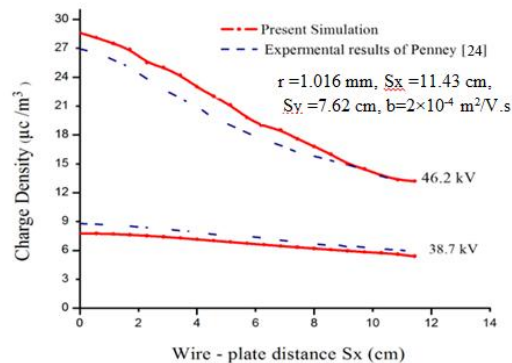


Fig.(10) Penney and Matick's experimental results of charge density distribution.

Fig.(9)Illustrate the present distribution of charge density along x-axis. It is clear that charge density distribution has higher value around the electrical discharge wire and the values decrease toward the collecting plate, and then the particle charging is reliable.fig.(10) Shows the distribution of charge density which explains comparison between results published by Penney and Matick's [24] and present simulation with different applied voltages and current densities. The values of charge density depends on the values of applied voltage and electric field intensity, the two cases in fig.(10) explain the distribution of charge density with high voltage 46.2kV and current density 0.689 mA/m²,and low voltage 38.7kV with current density0.226 mA/m²,the low voltage has slightly change. The experimental data very close to the simulation results and agreement is acceptable.

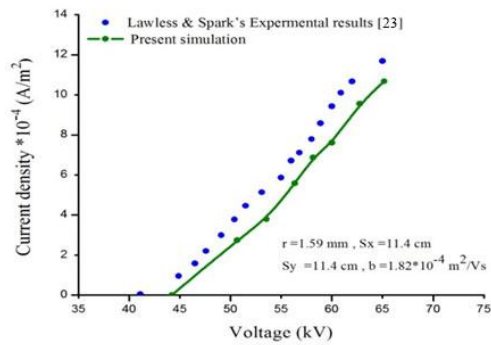


Fig.(11) Present simulation and experimental results of Lawless and Spark's

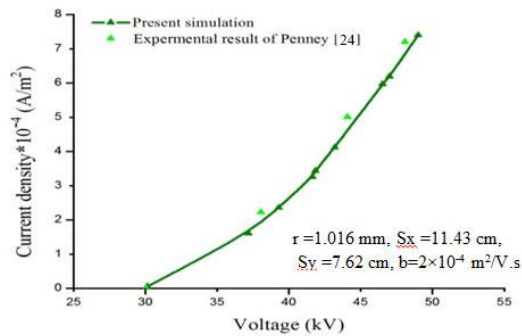


Fig.(12) present simulation and experimental results of Penney and Matick's.

The present dust free air model is validated with the two experimental results. For a model of WDEP exported by Lawless and Spark's with a discharging wire radius of 1.59 mm, wire-to-plate spacing S_x of 114.3 mm and wire to wire spacing S_y of 114.3 mm and mobility $= 2 \times 10^{-4} \text{ m}^2/\text{Vs}$. [23], there is quite agreement as compared to the present calculated value sare shown in fig.(11). Also it is very close between experimental results of Penney and Matick's [24] for input data: wire radius = 1.016 mm, wire –plate spacing = 11.43 cm, half wire to wire distance = 7.62 cm, mobility $= 2 \times 10^{-4} \text{ m}^2/\text{Vs}$. and our simulation, as shown in Fig.(12).

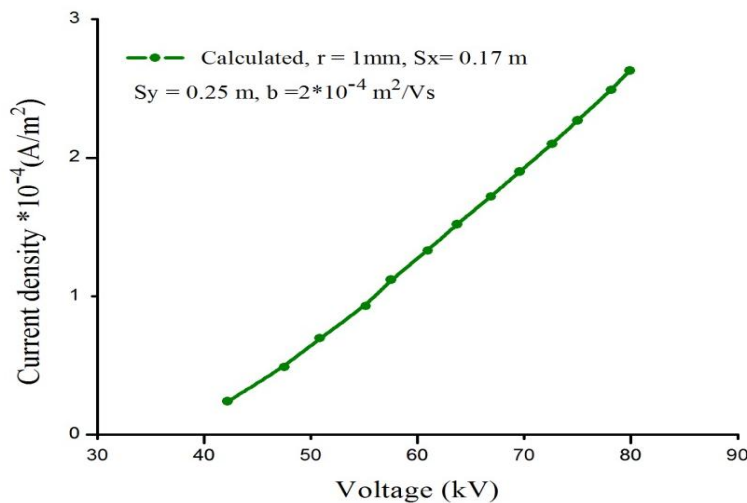


Fig. (13) V-I characteristics of ESP at Babylon cement plant.

The V-I curve of ESP is considered as a measurement of ESP efficiency, therefore Fig.(13) can be used to determine the efficiency of ESP at Babylon cement plant and the value for applied voltage and current density give a good tool for maintainance the ESP.

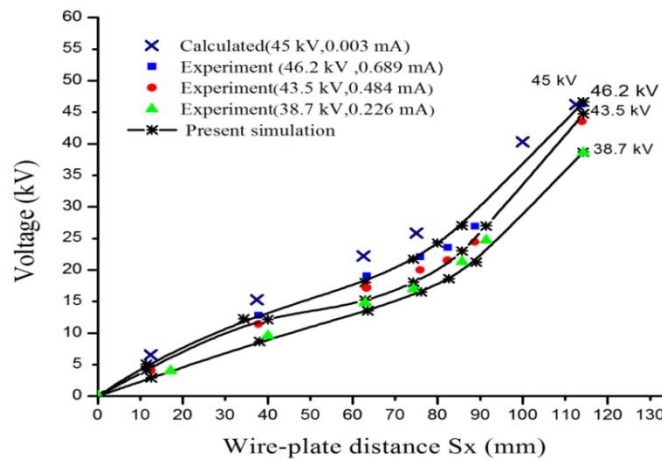


Fig. (14) Potential distribution of Penney and Matick's at different applied voltages ($r = 1.016$ mm, $S_x = 11.43$ cm, $S_y = 7.62$ cm, $b = 2 \times 10^{-4}$ m²/V s, $\delta = 1$, $f = 1$).

The inverse distribution of applied voltage is shown in fig. (14). The potential is zero at collecting plate and increase linearly along wire-plate distance until reach highest value at the point of corona discharge. All the curves have the same way for various values of applied voltages and current density; it is clear there are very close between experimental results [16] and present simulation for the same input data. The predicted curve also gives the same result. fig.(14) validated the first step of the model about the potential distribution between the electrical discharge and collecting plates and this distribution make corona discharge .

Table (1) the main electrical characteristics for ESP's at Babylon cement plant, Babylon, Iraq

Wire radius mm	Corona onset voltage kV	Applied voltage kV	Current density mA/m ²
1	16.404	67.8	0.098
1.1	17.323	68.8	0.099
1.2	18.210	69.2	0.100
1.3	19.069	70.0	0.101
1.4	19.904	71.6	0.102
1.5	20.715	84.8	0.203

Table (1) summarizes the main electrical characteristics for ESP predicated by our simulation, the corona onset voltage in an ESP influenced by the wire radius .for input data: wire –plate spacing =17cm, half wire to wire distance =25cm, mobility = 2×10^{-4} m²/vs.

Conclusion

The V-I characteristic of a dc precipitator at Babylon cement plant, neglecting the presence of fly ash, are calculated by a numerical procedure based on the Finite Difference Method, The ion charge density, the electric potential, and the electric field distributions are evaluated.

The V-I characteristic, obtained by means of the mathematical procedure described, is compared with the experimental one. The satisfactory agreement guarantees the reliability of the proposed mathematical model.

The model will be implemented for mantanice ESP at Babylon cement plant and considering the induced effect of the dust present in the flue gas, the back corona, and the dynamic corona originating from the application of pulsed-voltage energization to the electrostatic precipitators.

References

- [1] James H. Turner, Phil A. Lawless, Toshiaki Yamamoto, and David W. Coy, "Electrostatic Precipitator", U.S. Environmental Protection Agency, Research Triangle Park, NC 27709, 1995.
- [2] Kenneth Parker and Norman Plaks, "Electrostatic Precipitator (ESP) Training Manual", United States Environmental Protection Agency, EPA-600/R-04-072, 2004. H.S.Park,K.W Lee, Theoretical Model of electrostatic precipitat or S.H.Kim,
- [3] performance for collecting polydisperse particlesJournal of electrostatic,50,177-190 2001.
- [4] J.Anagnostopoulos andG.Bergeles, corona discharges simulation in wire-duct electrostatic precipitator, Journal of electrostatic 54,129-147,2002.
- [5] B.S. Rajanikanth and D. V. S. Sarma Modeling the Pre-Breakdown V-I Characteristics of an Electrostatic Precipitator, IEEE Transactions on Dielectrics and Electrical Insulation, Vol. 9, No. 1, February 2002.
- [6] B.S.Rajanikanthand N.Thirumaran,Prediction of pre-breakdown V-I characteristics of an electrostatic precipitator using a combined boundary element-finite difference approach, Fuel Processing Technology. v.76,159– 186 , 2002.[7] Anderson, Chance, Fargo, Hubbell, What is corona, Hubbell Power Systems, Inc., 2004.
- [8] Albert W Yuen, B.E. (Hons), ph. D thesis, University of New South Wales November, 2006.
- [9] NiloofarFarnoosh, ph. D thesis, The University of Western Ontario London, Ontario, Canada, 2011.
- [10] Dr. Philip D. Rack, Plasma Physics, Rochester Institute of Technology.
- [11] M.R. Talaie, M. Taheri, J. Fathikaljahi,A new method to evaluate the voltage–current characteristics applicable for a single-stage electrostatic precipitator,Journal of Electrostatics. v. 53 pp 221–233, 2001.

- [12] M. Abdel-Salam, A. Eid, Finite Element Simulation of Coronain Wire-Duct Precipitators, IEEE, 1383-1389, 2002.
- [13] Zakariya M. Al-Hamouz and Nabil S. Abuzaid, Numerical Computation of Collection Efficiency in Wire Duct Electrostatic Precipitators, IEEE, 1390-1396, 2002.
- [14] Zakariya Al-Hamouz, Amer El-Hamouz, Analysis of a wire-duct electrostatic precipitator under dust loading conditions, Energy Conversion and Management 52, 1235–1243, 2011.
- [15] B. S. Rajanikanth and M. V. Jayan, Simulation of Dust Loaded V-I characteristics of a Commercial Thermal Power Plant Precipitator, IEEE Transactions on Dielectrics and Electrical Insulation. v. 17, no. 1, 2010.
- [16] Zhuangbo Feng and Zhengwei Long, Voltage-current characteristics of a pin-plate system with different plate configurations, IOP Science, Journal of Physics, 2013.
- [17] Zhuangbo Feng, Zhengwei Long, and Qingyan Chen, Voltage-current characteristics of needle-plate system with different media on the collection plate, Journal of Electrostatics, 72, 129-135, 2014.
- [18] Fadhil K. Fuliful, A mathematical Model for Computing Effects of Back Corona in wire-duct Electrostatic Precipitators of Karbala Cement, Journal of Babylon University, v. 22, no. 1, 2012.
- [19] Nima Afshar-Mohajer, Yatit Thakker, Chang-Yu Wu Nicoleta Sorloaica-Hickman, Influence of Back Electrostatic Field on the Collection Efficiency of an Electrostatic Lunar Dust Collector, Aerosol and Air Quality Research, 14: 1333–1343, 2014
- [20] H. Ziedan, A. Sayed, A. Mizuno, and A. Ahmed, Onset Voltage of Corona Discharge in Wire-Duct Electrostatic Precipitators, International Journal of Plasma Environmental Science & Technology, v. 4, no. 1, 2010. [21] F.W. Peek Jr., Dielectric Phenomena in High Voltage Engineering, McGraw-Hill, New York, USA, 1929.
- [22] G. Cooperman, "A new voltage-current relation for low and high current densities", IEEE Trans. Indust. Appl. Soc., Vol. 17, pp. 236 – 239, 1981.
- [23] P.A. Lawless and L.E. Sparks, "A mathematical model for back corona in wire-duct precipitators", J. Appl. Physic, Vol. 51, pp. 242 – 256, 1980.
- [24] G.W. Penny and R.E. Matlick, "Potentials in DC corona fields", Trans. AIEE, part I, Vol. 79, pp. 91 – 99, 1960.